3D VOLUME DATA SEGMENTATION FROM SUPERQUADRIC TENSOR ANALYSIS

Sang Min Yoon and Arjan Kuijper
GRIS TU Darmstadt, Fraunhofer IGD & TU Darmstadt
Fraunhoferstrasse 5, Darmstadt, 64283, Germany

Keywords: 3D Model segmentation, Ellipsoidal representation, Diffusion tensor fields based similarity measure.

Abstract: The segmentation of 3D target objects into coherent subregions is one of the most important issues in computer graphics as it is applied in many applications, such as medical model visualization and analysis, 3D model retrieval and recognition, skeleton extraction, and collision detection. The goal of 3D segmentation is to separate the volume or mesh data into several subregions which have similar characteristics.
In this paper, we present an efficient and accurate 3D model segmentation methodology by merging and splitting the subregions in a 3D model. Our innovative 3D model segmentation system consists of two steps: *i*) the ellipsoidal decomposition of unorganized 3D object using properties of three dimensional second-order diffusion tensor fields, and *ii*) The iteratively merging and splitting of subregions of the 3D model by measuring the similarity between neighboring regions. Experimental results are conducted to evaluate the performance of our methodology using 3D models from well-known databases and 3D target objects that are reconstructed from image sequences.

1 INTRODUCTION

In the worlds of computer graphics, several mature methods for an automatic 3D visualization and analysis of real objects have been heavily studied. In particular, the segmentation of 3D target objects into coherent sub-regions has received many concerns in last few years because it is very useful in many applications, such as medical volume rendering and analysis, 3D shape retrieval and action recognition, skeleton extraction, and collision detection. The goal of 3D model segmentation is to separate the 3D data into mutually exclusive homogeneous subregions of interest.

Nevertheless, there is no standard formal definition of exact 3D model segmentation. Subdivided regions using segmentation methodologies are different according to their features and clustering techniques. Recently, Chen et al. (Chen et al., 2009) tried to compare the difference of the automatically segmented 3D models and human-visual perception based segmentation. For efficient segmentation of 3D volume data, extraction of robust features and a similarity measure between separated neighbor regions are needed. Previous research to segment 3D meshes which are composed with numerous triangles (Lien et al., 2006; Tierny et al., 2008) focused on their effort for novel clustering techniques in the the space of scalar or vector fields.

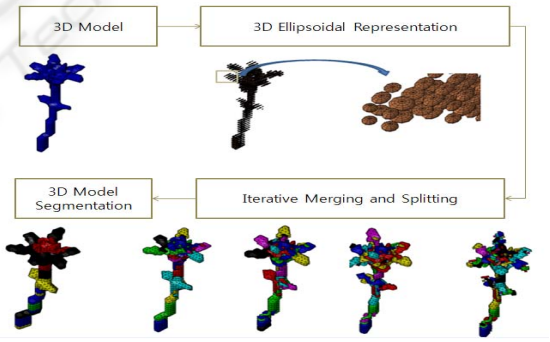

Figure 1: Flowchart of our proposed 3D object segmentation using the characteristics of the 3D ellipsoidal model.

In this paper, we present a 3D model segmentation methodology using an ellipsoidal representation of the 3D model in the space of diffusion tensor fields. Using the properties of diffusion tensor fields, we iteratively merge and split the subregions of 3D target objects. The eigen-features which come from diffusion tensor fields are used to measure the similarity between neighbor subregions. Figure 1 shows the total flowchart which we will explain in the paper using

Min Yoon S. and Kuijper A. (2010).
3D VOLUME DATA SEGMENTATION FROM SUPERQUADRIC TENSOR ANALYSIS.
In *Proceedings of the International Conference on Computer Graphics Theory and Applications*, pages 72-77
DOI: 10.5220/0002818800720077

the example 3D volume data.

Our main contributions are (1) the 3D ellipsoidal representation of the 3D volume/mesh model using the properties of diffusion tensor fields, (2) the iterative merging and splitting the neighboring regions by measuring the similarity of characteristics of diffusion tensorial features, and (3) the efficient and robust 3D segmentation for diverse models or reconstructed objects from multiple images without any constraints, prior knowledge, or assumptions on the 3D model.

2 PREVIOUS WORK

Our methodology has been motivated by the concept of superquadric representation of 3D models, 3D diffusion tensor fields and its applications, and 3D segmentation techniques. In this section, we survey the previous work which contributed significantly to the innovation within this area.

2.1 Superquadric Representation

The representation of a 3D model using superquadrics is used for visualizing its characteristics with only very few parameters cylinders, geons, superquadrics, etc. Superquadrics are a family of geometric solids, which can be interpreted as a generalized of basic quadric surfaces and solids. With only a few parameters, they can represent a large variety of standard geometric solids and smooth shapes. Superquadrics are also very efficient for representing three dimensional surface data. In contrast to a mesh representation of an object with thousands of triangles, the same object can be represented by a small set of superquadrics which are uniquely defined by 11 parameters per each voxel (Zhang et al., 2003).

2.2 Diffusion Tensor Fields

Most 3D volume segmentation and visualization methodologies are based on vector fields which are generated from a given image by different physical properties. Few works have investigated the extraction of features within resulting tensor fields. Basser et al. (Basser et al., 1994) presented their seminar work on diffusion tensor magnetic resonance imaging (DT-MRI). Using this new MRI modality, it was possible to qualify anisotropic properties of an imaged tissue by characterizing the water diffusion. In particular, Kindlmann (Kindlmann, 2004) presented a tensor based superquadric visualization method by mapping the tensor eigenvalues and eigenvectors to the orientation and shape of geometric primitives.

2.3 3D Model Segmentation

Segmentation techniques can be separated into classes in many ways according to different classification schemes, Shamir (Sharmir, 2006) surveyed the previously 3D segmentation of 3D volumes and separated the 3D segmentation problem into two types: as surface-type and part-type segmentation. Surface-type based segmentation is based on the decomposition of geometric primitives such as planes, cylindrical patches, and spherical parts (Wu and Levine, 2005; Attene et al., 2000). The part-type segmentation decomposes a 3D object into sub-meshes by segmenting a surface into connected components (Lien et al., 2006; Tierny et al., 2008). The segmentation algorithms used various approximating solutions such as K-means (Shlafman et al., 2002), region growing (Chazelle et al., 1997), hierarchical clustering (Garland et al., 2001; Inoue et al., 2001), graph-cuts (Katz and Tal, 2003), iterative clustering (Chevalier et al., 2003), and spectral analysis (Liu and Zhang, 2004).

3 SUPERQUADRIC DECOMPOSITION USING TENSORIAL FEATURES OF 3D MODEL

Previous 3D segmentation techniques are mainly based on mesh/triangle based 3D models in the space of vector or scalar transformations, because similarity measures within these spaces relate to the perception of the human eye. Nevertheless, tensorial maps contain and provide more information than scalar ones as to measure the similarity between neighbor regions. In this section, we decompose the 3D mesh models into 3D ellipsoidal models using the properties of three dimensional second-order symmetric diffusion tensor fields.

A tensor is the mathematical identification of a geometric or physical quantity whose analytic description consists of an array of numbers. The tensor field commonly defined as a topological representation of a 3D symmetric, second-order symmetric tensor field is shown as (Delarcelle and Hesselink, 1994):

$$T = \begin{pmatrix} T_{xx} & T_{xy} & T_{xz} \\ T_{yx} & T_{yy} & T_{yz} \\ T_{zx} & T_{zy} & T_{zz} \end{pmatrix}, \qquad (1)$$

where $T_{xy} = T_{yx}$, $T_{xz} = T_{zx}$, and $T_{yz} = T_{zy}$ since the order of differentiation is free, so that the tensor is a symmetric positive definite matrix. This matrix can

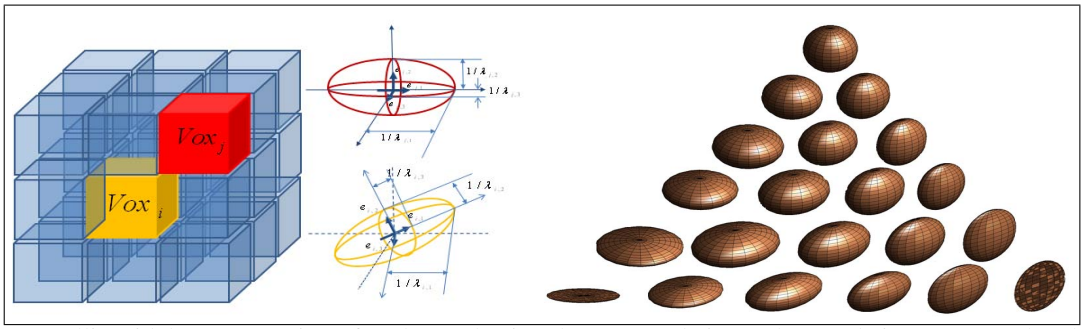

(a) 3D ellipsoidal representation of each voxel using the extracted eigenvalues and eigenvectors. (b) The superquadric tensor visualization as the change of the eigenvalues' values, giving rise to differently oriented ellipsoids.

Figure 2: The superquadric representation uses the eigenvalues and eigenvectors of the diffusion tensor fields which determine the scale and orientation of the superquadric model.

be reduced to principal axes by solving the characteristic equation

$$(T - \lambda_i \cdot \mathbf{I})\mathbf{e_i} = \mathbf{0}, \qquad (2)$$

where $\mathbf{I}$ is the identity matrix, λ_i are the eigenvalues of the tensor and e_i are the orthonormal eigenvectors ($i = 1,\ldots,3$). In this case, the tensor in each pixel can be represented by an ellipsoid, where the main axis lengths are proportional to the ordered eigenvalues λ_i ($\lambda_1 \geq \lambda_2 \geq \lambda_3 > 0$).

The evaluation of the tensor ellipsoidal geometrics and their properties is facilitated by an intuitive domain that spans all possible tensor shapes. Such a domain is afforded by the geometric anisotropy metrics of Kindlmann (Kindlmann, 2004). Given the non-negative tensor eigenvalues $\lambda_1, \lambda_2, \lambda_3$, the metrics quantifying the certainty with which a tensor is said to have a given shape are given by:

$$c_l = \frac{\lambda_1 - \lambda_2}{\lambda_1 + \lambda_2 + \lambda_3},\ c_p = \frac{2(\lambda_2 - \lambda_3)}{\lambda_1 + \lambda_2 + \lambda_3},\ c_s = \frac{3\lambda_3}{\lambda_1 + \lambda_2 + \lambda_3}.$$

The three metrics add up to unity, and define a barycentric parameterization of a triangular domain, with the extremes of linear, planar, and spherical shapes at the three corners. The barycentric shape space has been used as the domain of transfer functions for direct volume rendering of diffusion tensors, and as an intuitive basis of comparison between various anisotropy metrics. Figure 2 is a conceptual representation of volume data showing how the superquadric models can be represented with extracted eigenvalues and eigenvectors. The ratio between eigenvalues determines the shape of the superquadrics, their sum defines their scale and its principal eigenvector direction defines the rotation of the superquadrics as shown in Figure 2b. Using the basic principal direction of the superquadric representation method, we can visualize the 3D volume data into superquadrics. Figure 3 shows some examples of 3D models such as "horse" and "tool" and zooms in to see the detailed shape and orientation of each superquadric model.

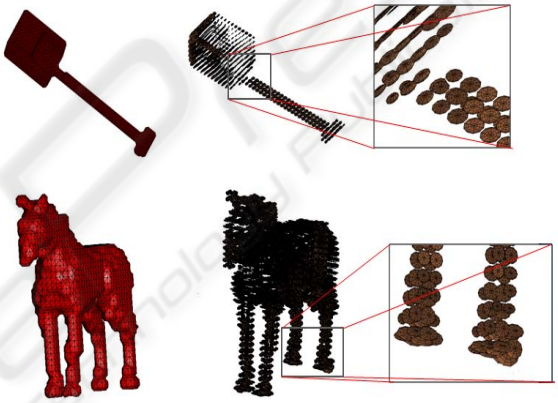

Figure 3: The superquadric representation of 3D volume data such as "tool" and "horse" using our proposed method.

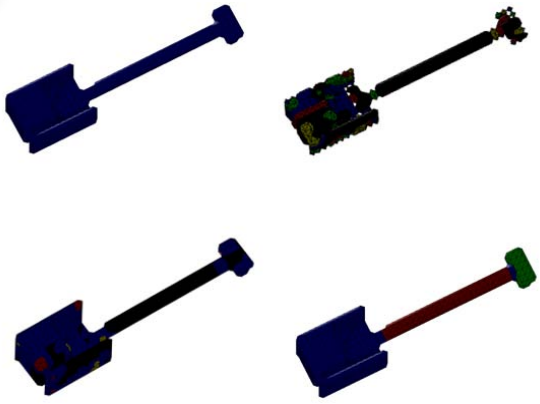

Figure 4: The process of segmenting the 3D target object using our proposed merging and splitting methodology. The unorganized 3D model is divided by its characteristics of tensorial features.

Figure 5: Some examples of 3D model segmentation using our approach using 3D models from the Princeton 3D model dataset.

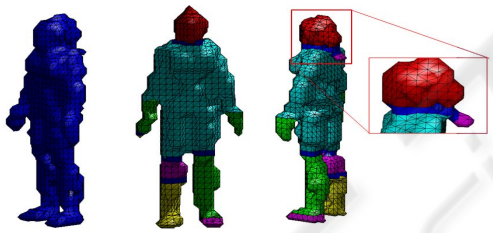

(a) Imported 3D volume data (b) Segmentation using our proposed method (c) Detail of the hair tail.

Figure 6: 3D model segmentation using our proposed methodology. Even though the hair tail is a small region, its superquadric characteristics are not similar to the neighboring regions and are therefore not merged with the neighbors.

4 ITERATIVE SEGMENTATION OF 3D MODEL

Various methods have been proposed to solve the problems of separating and clustering subregions of the 3D target object. In this section, we present the separation the unlabeled 3D model into segmented subregions using properties of the eigen-features. The degree of anisotropy of the ellipsoidal 3D model can be quantified in a single number called diffusion anisotropy index, or *fractional anisotropy* (FA), and is defined as follows:

$$FA = \sqrt{\frac{3[(\lambda_1-\lambda_{avg})^2+(\lambda_2-\lambda_{avg})^2+(\lambda_1-\lambda_{avg})^2]}{2(\lambda_1^2+\lambda_2^2+\lambda_3^2)}}, \quad (3)$$

where λ_{avg} is the average of λ_1, λ_2, and λ_3. The FA is used as feature to measure the similarity of neighbor voxels to segment the 3D model.
The 3D model segmentation procedure is as follows:

STEP0 : Initially, the numbers of subregions of the human body model is equal to the number of voxels of the 3D human model. Calculate $FA_{ij} = \sqrt{(FV_i - FV_j) \times (FV_i - FV_j)}$, where FV_i and FV_i are FA of voxel i and j, respectively.

STEP1 : Progressively merge the neighbor voxels if FA_{ij} is less than threshold and recalculate the average FA of the merged subregions, $FA_{sub} = \frac{1}{n}\sum_{k=1}^{n} FA_k$, where the merged subregion which have n voxels. The voxels i and j are splitted if FA_{ij} exceeds the threshold.

STEP2 : Repeat **STEP1** until there are no subregions whose the FA_{sub} is less than threshold.

5 EXPERIMENTS

We implemented our proposed 3D segmentation methodology using the superquadric features in the space of diffusion tensor fields and conducted experiments on a standard PC with a Pentium 4 1.2 GHz CPU. First, we have tested our methodology using the Princeton 3D model database. They provided the 3D models in Object File Format (OFF) with a polygonal geometry of the model. We have converted the objects to a voxel based model which has a 128x128x128 voxel size. Figure 5 shows some examples, such as an animal, a tool, and a guitar. We displayed the segmented regions with various colors. Figure 6 shows a Princeton database example in more detail. As shown in Figure 6(d), a small subregion is correctly segmented from the neighboring regions because its tensorial characteristics are very different from the neighbor regions.

We also tested our algorithms on 3D reconstructed objects obtained from multiple images. The images came from the HumanEva database. We first reconstructed the target object from multiple images by image based visual hulls using provided camera calibration data and statistics of background modeling with 128x128x128 voxel size volumes. We adapted our method to the 3D reconstructed model as shown in Figure 7. Using the extracted silhouette of fore-

(a) Input images of multiple cameras from the HumanEva dataset.

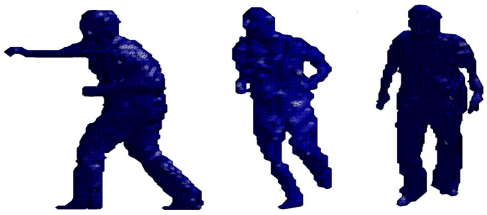

(b) 3D reconstructed object from the HumanEva dataset.

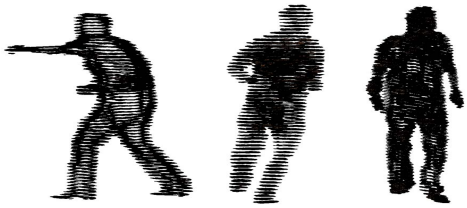

(c) 3D ellipsoidal representation of the target objects.

(d) 3D segmentation into distinct parts using our proposed approach.

Figure 7: 3D model segmentation by using 3D reconstruction from multiple images.

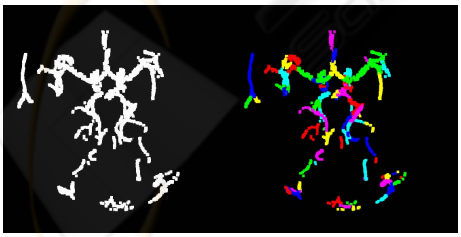

(a) Unlabeled 3D human brain volume data whose resolution is 512x512x512. (b) Segmented human brain volume data by using our approach.

Figure 8: Medical volume segmentation and rendering.

ground and camera calibration information, we reconstructed the target object using Image-Based Visual Hull (IBVH) (Matusik et al., 2000).

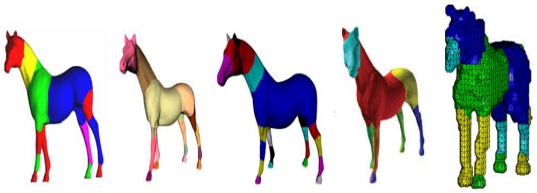

(a) 3D segmentation of Zhang et al., (b) 3D segmentation of Lien et al., (c) 3D segmentation of Tierny et al., (d) consistent segmentation, (e) our proposed 3D segmentation using iterative merging and splitting.

Figure 9: Some examples of 3D model segmentation using our approach from the 3D models from Princeton' 3D model dataset.

Our 3D model segmentation technique also applied to medical volume understanding and analysis area. Figure 8 shows the segmented human brain volume data using our approach. Figure 8a is the unlabeled 3D MRI data whose resolution is 512x512x512. We can segment the 3D medical volume data into several subregions which have similar tensorial characteristic. Our approach does not require priori information to segment the 3D volume data, we can apply to various target objects which have high-degree of freedom.

We compared our methodology to several other approaches, see for example Figure 9. It contains the approaches by Zhang et al. (Zhang et al., 2003) in Figure 9a, Lien et al. (Lien et al., 2006) in Figure 9b, Tierny et al. (Tierny et al., 2008) in Figure 9c, and the consistent segmentation in Figure 9d. The 3D "horse" model is commonly divided into a main body part, 4 legs, a neck, and a head. Especially the 3D segmentation of Tierny et al. (Tierny et al., 2008) has many subregions. Note that the intention of our approach is not to specific segment the target object as shown in Figure 8, but a generating distinct subregions. Subregions are divided into smaller region if their tensorial characteristics are very different to the neighborhood as shown in Figure 6. Previous approaches are based on the 3D mesh models which are composed of numerous triangles, but our 3D models are only based 128x128x128 voxel sized volumes. Our results can be used to define the subregions in the smooth triangulated versions.

6 CONCLUSIONS AND FUTURE WORK

In this paper, we presented a 3D volume segmentation methodology using tensorial properties of dif-

fusion tensor field. The superquadric model using the properties of the 3D second-order diffusion tensor fields efficiently visualize the characteristics of the 3D model using only few parameters. We cluster the 3D volume data by iteratively merging and splitting the neighboring regions using the similarity measure of tensorial features.

Experiments of 3D segmentations of the imported 3D models and 3D reconstructed objects from multiple image sequences, we show that our proposed system is very efficient and robust in separating the 3D volume data into several subregions which have similar tensorial characteristics. Our 3D model segmentation is very useful in 3D deformable object motion analysis and medical volume visualization.

This methodology provides a basis for the segmentation and tracking of deformable object segments. Hence, our future work will focus on consistent 3D model segmentation optimized for speed and performance as soon as qualitative benchmarks can be given. The exploitation of additional semantics together with our methodology could lead to a fast 3D segmentation approach. Vice versa, the derivation of semantical metadata for subregions of a 3D object will also be addressed in future work.

REFERENCES

Attene, M., Falcidieno, B., Spagnuolo, M., 2000. Hierarchical mesh segmentation bsed on fitting primitives. *The Visual Computer.*

Basser, P. J., Mattiello, J., and Le Bihan, D., 1994. MR diffusion tensor spectroscopy and imaging. *Biophys Journal.*

Chazelle, B., Dobkin, D., Shourhura, N., and Tal, A., 1997. Strategies for polyhedral surface decomposition: An experimental study. *Computational Geometry: Theory and Applications.*

Chevalier, L., Jaillet, F., and Baskurt, A., 2003. Segmentation and superqadric modeling of 3D object *WSCG.*

Chen, X., Golovinskiy, A., and Funkhouser, T., 2009. A Benchmark for 3D Mesh Segmentation *SIGGRAPH.*

Delarcelle, T., and Hesselink, L., 1994. The topology of symmetric, second-order tensor fields. *In proceeding of IEEE Visualization.*

Golovinskiy, A., and Funkhouser, T., 2009. Consistent Segmentation of 3D Models. *Computer and Graphics.*

Garland, M., Willmott, A., and Heckbert, P., 2001. Hierarchical face clusterig on polygonal surfaces. *In ACM Symposium on Interactive 3D Graphics.*

Inoue, K., Takayuki, I., Atsushi, Y., Tomotake, F., and Kenji, S., 2001. Face clustering of a large-scale card model for surface mesh generation. *Computer-Aided Design.*

Kindlmann, G., 2004. Superquadric tensor Glyph. *Joint Eurographics- IEEE TCGV Symposium on Visualization.*

Katz, S., and Tal, A., 2003. Hierarchical mesh decomposition using fuzzy clustering and cuts. *In SIGGRAPH.*

Lange, K., and Carson, R., 1984. EM reconstruction algorithms for emission and transmission tomography. *Journal of Computer Assisted Tomography.*

Leonardis, A., Jaklic, A., and Solina, F., 1997. Superquadrics for segmenting and modeling range data. *IEEE trans. on PAMI.*

Lien, J.-M., Keyser, J., and Amato, N. M., 2006 Simultanious shape decomposition and skeletonization. *In proceeding of ACM Symposium on Solid and Physical Modeling.*

Liu, R., Zhang, H., 2004. Segmentation of 3D meshes through spectral clustering. *In proceeding of Pacific Conference on Computer Graphics and Applications.*

Matusik, M., Buehler, C., Raskar, R., Gortler, S. J., and Mcmillan, L., 2000. Image-based visual hulls t. *SIGGRAPH.*

Moller, T., 1997. A fast triangle-triangle intersection test. *Journal of Graphics Tools.*

Sharmir, A., 2006. Segmentation and Shape Extraction of 3D Boundary Meshes. *In proceeding of Eurographcs, State of The Art Report.*

Shlafman, S., Tal, A., and Katz, S., 2002. Metamorphosis of polyhedral surfaces using decomposition. *In proceeding of Eurographics.*

Tierny, J., Vandeborre, J.-P., and Daoudi, M., 2008. Fast and precise kinematic skeleton extraction of 3D dynamic meshes. *In proceeding of CVPR.*

Wu, J., Levine, M., 2005. Structure recovery via hybrid variational surface approximation. *In proceeding of Eurographics.*

Zhang, Y., Koschan, A., and Abidi, M., 2003. Superquadrics based 3D object representation of automotive parts utilizing part decomposition. *In proceeding of International Conference on Qaulity control by Artifical Vision.*